Generalized Model of Blood Flow in a Vertical Tube with Suspension of Gold Nanomaterials: Applications in the Cancer Therapy

Anees Imtiaz[1], Oi-Mean Foong[2], Aamina Aamina[1], Nabeel Khan[1], Farhad Ali[3, 4, *] and Ilyas Khan[5]

Abstract: Gold metallic nanoparticles are generally used within a lab as a tracer, to uncover on the presence of specific proteins or DNA in a sample, as well as for the recognition of various antibiotics. They are bio companionable and have properties to carry thermal energy to tumor cells by utilizing different clinical approaches. As the cancer cells are very smaller so for the infiltration, the properly sized nanoparticles have been injected in the blood. For this reason, gold nanoparticles are very effective. Keeping in mind the above applications, in the present work a generalized model of blood flow containing gold nanoparticles is considered in this work. The blood motion is considered in a cylindrical tube under the oscillating pressure gradient and magnetic field. The problem formulation is done using two types of fractional approaches namely CF (Caputo Fabrizio) and AB (Atangana-Baleanue) derivatives, whereas blood is considered as a counter-example of Casson fluid. Exact solutions of the problem are obtained using joint Laplace and Hankel transforms, and a comparative analysis is made between CF and AB. Results are computed in tables and shown in various plots for embedded parameters and discussed. It is found that adding 0.04-unit gold nanoparticles to blood, increase its heat transfer rate by 4 percent compared to regular blood. It is also noted that the heat transfer can be enhanced in the blood with memory.

Keywords: Gold nanoparticles, heat transfer enhancement, blood flow, Casson fluid, AB, CF fractional derivatives.

[1] Department of Mathematics, City University of Science and Information Technology, Peshawar, Pakistan.
[2] Computer and Information Sciences Department, Universiti Teknologi PETRONAS, Seri Iskandar, Malaysia.
[3] Computational Analysis Research Group, Ton Duc Thang University, Ho Chi Minh, Vietnam.
[4] Faculty of Mathematics and Statistics, Ton Duc Thang University, Ho Chi Minh, Vietnam.
[5] Department of Mathematics, College of Science Al-Zulfi, Majmaah University, Al-Majmaah, 11952, Saudi Arabia.
[*] Corresponding Author: Farhad Ali. Email: farhad.ali@tdtu.edu.vn.
Received: 06 May 2020; Accepted: 12 June 2020.

1 Introduction

Nanoscience is the study of materials at atomic, molecular and macromolecular scales where physio-chemical residences might also differ notably from those at a larger particulate scale. The high-quality improvement of nanotechnology within the last decade promises innovative innovations inside the medical subject, beginning a big spectrum of opportunities and demanding situations [Leech and Scott (2017)]. Nanomaterials are considered powerful gear to reach healing targets in any other case difficult to reap via commonplace medical protocols. An awesome instance is using nanoparticles as drug providers and diagnostic probes for strong cancers [Ho, Pfeffer and Singh (2017)]. Most human cancers are complicated sicknesses resulting from genomic volatility and accretion of a couple of molecular changes. Existing indicative and prophetic taxonomies do no longer imitate the entire clinical heterogeneity of tumors [Pavlova and Thompson (2016)]. Recent studies have advanced efficient nanoparticles that are allied to biological molecules which include peptides and nucleic acids [Ashizawa and Cortes (2015); Saallah and Lenggoro (2018); Agostinelli, Vianello, Magliulo et al. (2015); Rudramurthy and Swamy (2018)]. In medical sciences, different nanoparticles such as magnetic particles and gold, have been studied for various clinical purposes, like magnetic particles and gold. In this study the gold nanoparticle has been considered, the question is why?

The use of gold compounds in modern medicinal drugs commenced with the invention in 1890 by Robert Koch using gold cyanide that turned into bacteriostatic in the direction of the tubercle bacillus [Herzog (1998)]. Gold metallic nanoparticles are generally used within the lab as a tracer, to stumble on the presence of specific proteins or DNA in a sample as well as for the recognition of various antibiotics like streptomycin and neomycin [Tomar and Garg (2013); Wang (2003)]. Researchers have these days used gold nanoparticles for figuring out one of a kind lesson of microorganisms. Gold nanoparticles are clean to synthesize, they are biocompatible and possess optical houses, inclusive of floor plasmon resonance leading to a narrow optical absorption band inside the visible/infrared spectrum relying on length and shape of AuNP. When they are injected in the bloodstream, the particles have interaction with blood proteins and biomolecules producing a biological interface at the surface, frequently called “corona”. The formation of such protein corona is a dynamic manner [Shilo, Berenstein, Dreifuss et al. (2015); Daniel and Astruc (2004)].

To stumble on and kill cancer cells, a unique sort of nanoparticles was used. However, amongst them, the gold nanoparticle has accomplished a distinguishing function. Ikram et al. [Ikram, Jamil, Ahmad et al. (2019)] have these days mentioned about capacity use of GNPs in photothermal destruction of tumours. Kong et al. [Kong, Zhang, Li et al. (2017)] used gold nanoparticles in drug delivery applications. Abdelhalim et al. [Abdelhalim and Jarrar (2011)] check out the particle-size impact of GNPs at the renal tissue and try to cope with their ability toxicity. Hussein et al. [Hussein, Sultan and Yaseen (2016)] examine the efficacy of photothermal therapy via the use of gold nanoparticles with laser irradiation on two cancer mobile traces *in vitro*. Iancu [Iancu (2013)] illustrates the modern-day achievements inside the applications of gold nanoparticles as photothermal retailers against human cancers. Yao et al. [Yao, Zhang, Wang et al. (2016)] show that

GNPs have not any inherent cytotoxicity possessions in human cancer cellular strains *in vitro* and GNPs launch warmth in a focused outside RF area.

Fractional derivatives are numerously used to investigate rheological properties in fluid mechanics. These derivatives have played a vital role in engineering and mathematical sciences and the world of fractional calculus, many mathematicians and researchers gave their contribution. In the present era of research, non-integer ordered derivatives are an effective and useful tool in physical situations. Fractional calculus produces more reliable, stable and effective mathematical models of physical problems in the area of chemistry, bioengineering and dynamics than classical calculus. Memory and hereditary properties of a fluid can be measured more accurately through fractional-order calculus instead of conventional order calculus. For an instant, fractional derivatives are used in bio-rheology, astrophysics, biophysics, thermodynamics, plasma physics, traveling wave solutions, optics and electromagnetism [Owolabi and Atangana (2019)]. Nowadays the two main definitions of Atangana and Baleanue (AB) and CF fractional derivatives are very famous in theoretical as well as experimental works. Owolabi et al. [Owolabi and Atangana (2018)] used the AB fractional derivative in Chaotic problems by the Adams Bashford method. Atangana [Atangana (2017a)] gave a new model of Darcy scale in a dual medium flow also gave a new numerical scheme in fractal fractional operators. Tremendous work has been given by Atnagana [Atangana (2017b)] in the field of Geohydrology using the fractional derivative. Atangana [Atangana (2016)] gives some new definitions of fractional derivatives related to Laplace and Fourier transforms and also gave a new model for real-world problems. Ali et al. [Ali, Yousaf, Khan et al. (2019)] used the definition of AB fractional derivative in blood flow with magnetic particles in cylindrical coordinates.

The above literature shows that numerous experimental articles on GNP's with blood and Fractional derivatives have been published, however, such types of theoretical studies, particularly on exact analysis, are scarce. To the best of our knowledge, no attempt has been found in which the exact solutions are presented for the blood flows in arteries with Gold nano-particles and heat transfer in a cylindrical domain using two integer order newly developed fractional models (Atangana-Baleanue) and (Caputo-Fabrizio) fractional derivative models. Since the blood flows in arteries and it is a Biomagnetic fluid [Ali, Imtiaz, Khan et al. (2018)], therefore cylindrical tube in the vertical direction is chosen as a physical model of the present problem. More exactly, in the present paper, the two well-known fractional models have been developed and the effect of GNPs in blood has been investigated. Since the blood has been considered so it is very necessary to take the pressure gradient in oscillatory form into account. The novelty of this problem is that a comparative analysis of Caputo-Fabrizio et al. [Atangana and Baleanue (2016)] fractional models have been considered with a transversely applied magnetic field. The two fractional models have been developed with the appropriate initial and boundary conditions the exact solutions have been obtained using the joint Laplace and Hankel transformations.

2 Blood flow mathematical model

The blood flow is considered in a vertical cylindrical tube of the radius $R_0\ \left(r_1,\theta_1,z\right)$ with the uniformly distributed gold nanoparticles. The uniform magnetic field applied transversely to the flow direction and the induced magnetic field is ignored for a small value of Reynold number [Srinivas and Kothandapani (2009)] as shown in Fig. 1. Blood flow is due to the uniform motion of the cylinder and buoyancy forces. Initially, the fluid, as well as the cylinder both, are stationary and the temperature is T_∞. At $t_1 = 0^+$, the temperature rises to T_w.

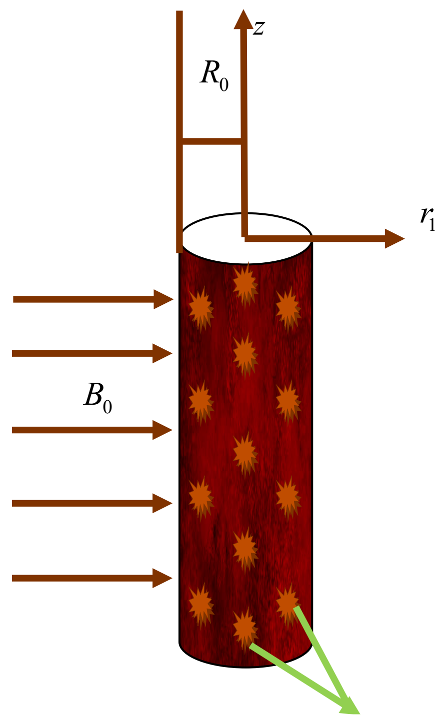

Figure 1: Flow configuration [Ali, Imtiaz, Khan et al. (2018)]

Under the above assumptions, the governing equations for the prescribed study as given by Oztop et al. [Oztop and Abu-Nada (2008)]

$$\left(\frac{\partial u(r_1,t_1)}{\partial t_1}\right) = -\frac{1}{\rho_{nf}}\frac{\partial p}{\partial z} + \frac{\nu_{nf}}{\gamma_0}\left(\frac{\partial^2 u(r_1,t_1)}{\partial r_1^2} + \frac{1}{r_1}\frac{\partial u(r_1,t_1)}{\partial r_1}\right) - \frac{\sigma_{nf} B^2{}_0}{\rho_{nf}} u(r_1,t_1) \tag{1}$$

$$\pm g(\beta\rho)_{nf}\left(T - T_\infty\right),$$

the pressure gradient of the oscillation form Aman et al. [Aman, Khan, Ismail et al. (2018)] is given by

$$-\frac{\partial p}{\partial z} = P_0 + P_1 cos\omega t_1, \tag{2}$$

here $u(r_1,t_1)$ is the blood velocity.

The energy equation is specified for the cylindrical coordinates is given by Ali et al. [Ali, Imtiaz, Khan et al. (2018)]:

$$\frac{\left(\rho c_p\right)_{nf}}{k_{nf}}\frac{\partial T(r_1,t_1)}{\partial t_1}=\frac{\partial^2 T(r_1,t_1)}{\partial r_1^2}+\frac{1}{r_1}\frac{\partial T(r_1,t_1)}{\partial r_1};\quad t_1>0, r_1\in\left(0,R_0\right), \tag{3}$$

subjected to the initial and boundary conditions

$$\left.\begin{array}{l} u\left(r_1,0\right)=0 \quad , \quad u\left(R_0,t_1\right)=0 \ , \\ T\left(r_1,0\right)=T_\infty \quad , \quad T\left(R_0,t_1\right)=T_w \\ \left.\dfrac{\partial u}{\partial r_1}\right|_{r_1=0}=0 \end{array}\right\}, \tag{4}$$

$$\left.\begin{array}{l} \rho_{nf}=\left(1-\phi\right)\rho_f+\phi\rho_s,\ \mu_{nf}=\mu_f\left(1-\phi\right)^{-2.5},\ \left(\rho\beta\right)_{nf}=\left(1-\phi\right)\left(\rho\beta\right)_f+\phi\left(\rho\beta\right)_s, \\ \left(\rho c_p\right)_{nf}=\left(1-\phi\right)\left(\rho c_p\right)_f+\phi\left(\rho c_p\right)_s,\quad \sigma_{nf}=\sigma_f\left[1+\dfrac{3\left(\sigma-1\right)\phi}{\left(\sigma+2\right)-\left(\sigma-1\right)\phi}\right], \\ \sigma=\dfrac{\sigma_s}{\sigma_f},\quad k_{nf}=k_f\left[\dfrac{k_s+2k_f-2\phi\left(k_f-k_s\right)}{k_s+2k_f+\phi\left(k_f-k_s\right)}\right],\gamma_0=\left(1+\dfrac{1}{\gamma}\right) \end{array}\right\}, \tag{5}$$

According to Oztop et al. [Oztop and Abu-Nada (2008)], the spherical shape NP model has been considered and the thermophysical properties of base fluid and nanoparticle are given in Tab 1.

Table 1: Thermophysical properties of blood and gold [Aman, Khan, Ismail et al. (2018); Hatami and Ganji (2014)]

Material	Symbol	ρ (Kg/m^3)	c_p(J/KgK)	k(W/mK)
Blood	-	1050	3617	0.52
Gold	Au	19300	129	318

Introducing the following dimensionless quantities

$$r_1^*=\frac{r}{R_0},\tau_1^*=\frac{\nu t_1}{R_0^{\,2}},e_1=\frac{u}{u_0},\theta=\frac{T-T_\infty}{T_w-T_\infty},\xi_0^*=\frac{P_0R_0^{\,2}}{\mu u_0},\xi_1^*=\frac{P_1R_0^{\,2}}{\mu u_0}, \tag{6}$$

into Eqs. (1)-(4), we get (dropping out star notation):

$$\frac{\partial e_1(r_1,\tau_1)}{\partial \tau_1}=\frac{(\xi_0+\xi_1\cos\omega\tau_1)}{\phi_1}+\gamma_1\left(\frac{\partial^2 e_1(r_1,\tau_1)}{\partial r_1^2}+\frac{1}{r_1}\frac{\partial e_1(r_1,\tau_1)}{\partial r_1}\right) \tag{7}$$
$$-Me_1(r_1,\tau_1)\pm Gr\theta(r_1,\tau_1),$$

$$\frac{\partial \theta(r_1,\tau_1)}{\partial \tau_1}=b_o\left(\frac{\partial^2 \theta(r_1,\tau_1)}{\partial r_1^2}+\frac{1}{r_1}\frac{\partial \theta(r_1,\tau_1)}{\partial r_1}\right);\quad r_1\in(0,1),\ \tau_1>0, \tag{8}$$

$$\left.\begin{array}{ll} e_1(r_1,0)=0 & ,\ \theta(r_1,0)=0 \\ e_1(1,\tau_1)=1 & ,\ \theta(1,\tau_1)=1 \\ \left.\frac{\partial e_1}{\partial r_1}\right|_{r_1=0}=0 & \end{array}\right\}, \tag{9}$$

with

$$Gr_1=\frac{\phi_3}{\phi_1}Gr,b_0=\frac{\lambda_f}{\Pr\phi_4},\gamma_1=\frac{1}{\gamma_0(1-\phi)^{2.5}\phi_1},M=\frac{\sigma_f R_0^2 B_0^2}{\rho_f \nu},M_1=\frac{\phi_2}{\phi_1}M,$$

2.1 Caputo-fabrizio fractional model and its solution

In fractional form, Eqs. (7) and (8) can be written as:

$${}^{CF}\wp_t^{\alpha} e_1(r_1,\tau_1)=\frac{(\xi_0+\xi_1\cos\omega t_1)}{\phi_1}+\gamma_1\left(\frac{\partial^2 e_1(r_1,\tau_1)}{\partial r_1^2}+\frac{1}{r_1}\frac{\partial e_1(r_1,\tau_1)}{\partial r_1}\right)$$
$$-M_1 e_1(r_1,\tau_1)\pm Gr\theta(r_1,\tau_1), \tag{10}$$
$${}^{CF}\wp_t^{\alpha}\theta(r_1,\tau_1)=b_0\left(\frac{\partial^2\theta(r_1,\tau_1)}{\partial r_1^2}+\frac{1}{r_1}\frac{\partial\theta(r_1,\tau_1)}{\partial r_1}\right), \tag{11}$$

Here $\wp_t^{\alpha}s(t)=\dfrac{1}{1-\alpha}\int_0^{\tau}\exp\left(\dfrac{-\alpha(\tau-t)}{1-\alpha}\right)f^{/}(\tau)dt,\ for\ 0<\alpha<1$ shows the Caputo-Fabrizio time-dependent fractional-order derivative.

For the solution of Eqs. (10)-(11) using nondimensional IBC's from (9) and the Laplace and Hankel transformations are utilized.

2.1.1 Solution of the energy equation

By applying the Laplace transform to Eq. (8), we get

$$\frac{a_0 q_1}{q_1 + a_1}\bar{\theta}(r_1, q_1) = b_0\left(\frac{\partial^2 \bar{\theta}(r_1, q_1)}{\partial r_1^2} + \frac{1}{r_1}\frac{\partial \bar{\theta}(r_1, q_1)}{\partial r_1}\right). \tag{12}$$

where $\bar{\theta}(r,q)$ is the Laplace transform of $\theta(r,t)$, $a_0 = \dfrac{1}{1-\alpha}$; $\alpha \neq 1$ and $a_1 = a_0\alpha$.

Now applying the Hankel transform of order zero and using the transformed condition, we get:

$$\overline{\theta_H}(r_{1n}, q_1) = \frac{J_1(r_{1n})}{r_{1n} q_1} - \frac{a_{5n}\, r_{1n}\, J_1(r_{1n})}{r_{1n}^{\ 2}\left(q_1 + a_{4n}\right)}, \tag{13}$$

where $a_2 = \dfrac{a_0}{b_0}, a_{3n} = a_2 + r_{1n}^{\ 2}, a_{4n} = \dfrac{a_1 r_{1n}^{\ 2}}{a_{3n}}, \dfrac{a_1}{a_{3n} a_{4n}} = \dfrac{1}{r_{1n}^{\ 2}}, a_{5n} = \dfrac{a_2}{a_2 + r_{1n}^{\ 2}}.$

Here

$\bar{\theta}_H\left(r_{1n}, q_1\right) = \int_0^1 r_1\, \bar{\theta}\left(r_{1n}, q\right) J_0\left(r_1 r_{1n}\right) dr_1$ is the Hankel transformation of the function $\bar{\theta}\left(r_1, q_1\right)$

Now by the Laplace transform to Eq. (13), yields

$$\overline{\theta_H}(r_{1n}, \tau_1) = \frac{J_1(r_{1n})}{r_{1n}} - \frac{a_5\, r_{1n}\, J_1(r_{1n})}{r_{1n}^{\ 2}}\exp\left(-a_4\tau_1\right), \tag{14}$$

which upon inverse Hankel transform results:

$$\theta(r_1, \tau_1) = 1 - 2\sum_{n=1}^{\infty}\frac{J_0(r r_{1n}) r_{1n} a_5}{r_{1n}^{\ 2}\, J_1(r_{1n})}\exp\left(-a_4\tau_1\right). \tag{15}$$

2.1.2 Solution of the velocity distribution

The Laplace transform of Eq. (10), yields

$$\left(\frac{a_0 q_1}{q_1 + a_1} + M_0\right)\overline{e_{1H}}\left(r_1, q_1\right) = \gamma_1\left(\frac{d^2 \bar{e}(r_1, q_1)}{\partial r_1^2} + \frac{1}{r_1}\frac{d\bar{e}(r_1, q_1)}{\partial r_1}\right) + Gr_1\,\bar{\theta}(r_1, q_1). \tag{16}$$

and the finite Hankel transform of Eq. (16) with boundary condition we get:

$$\begin{aligned}\left(\frac{a_0 q_1}{q_1 + a_1} + M_1\right)\overline{e_{1H}}\left(r_{1n}, q_1\right) &= \gamma_1\begin{pmatrix} -r_{1n}^{\ 2}\,\overline{e_H}\left(r_{1n}, q_1\right) \\ +r_{1n} J_1(r_{1n})\,\bar{e}(1, q_1)\end{pmatrix} \\ &+ \frac{1}{\phi_1}\left(\frac{\xi_0}{q_1} + \frac{\xi_1}{q_1^{\ 2} + \omega^2}\right)\frac{J_1\left(r_{1n}\right)}{r_{1n}} + Gr_1\,\overline{\theta}_H(r_{1n}, q_1).\end{aligned} \tag{17}$$

using $\overline{e}(1,q_1)=\dfrac{1}{q_1}$, Eq. (17) becomes:

$$\overline{e_{1H}}\left(r_{1n},q_1\right)=\begin{pmatrix}\dfrac{\gamma_1 r_{1n}J_1(r_{1n})}{q_1}+Gr_1\,\overline{\theta}_H(r_{1n},q_1)\\ +\dfrac{1}{\phi_1}\left(\dfrac{\xi_0}{q_1}+\dfrac{\xi_1}{q_1^{\,2}+\omega^2}\right)\dfrac{J_1\left(r_{1n}\right)}{r_{1n}}\end{pmatrix}\left(\frac{q_1+a_1}{\begin{matrix}\left(a_0+\gamma_1 r_{1n}^{\;2}+M_1\right)q_1\\ +\left(\gamma_1 r_{1n}^{\;2}+M_1\right)a_1\end{matrix}}\right). \tag{18}$$

Eq. (18) is simplified in the following form:

$$\overline{e_{1H}}\left(r_{1n},q_1\right)=F_{0n}\left(q_1\right)+F_{1n}\left(q_1\right)+F_{2n}\left(q_1\right), \tag{19}$$

where

$$F_{0n}\left(q_1\right)=\frac{\gamma_1 r_n J_1(r_n)}{q_1}\left(\frac{q_1+a_1}{\left(a_0+\gamma_1 r_n^{\;2}+M_0\right)q_1+\left(\gamma_1 r_{1n}^{\;2}+M_0\right)a_1}\right)$$

$$F_{1n}\left(q_1\right)=Gr\,\overline{\theta}_H(r_{1n},q_1)\left(\frac{q_1+a_1}{\left(a_0+\gamma_1 r_{1n}^{\;2}+M_0\right)q+\left(\gamma_1 r_{1n}^{\;2}+M_0\right)a_1}\right)$$

$$F_{2n}\left(q_1\right)=\frac{1}{\phi_1}\left(\frac{\xi_0}{q_1}+\frac{\xi_1}{q_1^{\,2}+\omega^2}\right)\frac{J_1\left(r_{1n}\right)}{r_{1n}}\left(\frac{q_1+a_1}{\left(a_0+\gamma_1 r_{1n}^{\;2}+M_0\right)q_1+\left(\gamma_1 r_{1n}^{\;2}+M_0\right)a_1}\right).$$

$F_{0n}\left(q_1\right)$ is further simplified as:

$$F_{0n}\left(q_1\right)=\frac{J_1(r_{1n})}{r_n\left(q_1\right)}+\frac{J_1(r_{1n})}{r_{1n}}\left(\frac{c_{8n}}{q_1}+\frac{c_{9n}}{q_1+c_{3n}}\right), \tag{20}$$

where

$c_{7n}=\dfrac{c_{4n}}{c_{1n}}$, $c_{6n}=\dfrac{c_{5n}}{c_{4n}}$, $c_{5n}=\gamma_1 r_{1n}^{\;2}a_1-c_{3n}$, $c_{4n}=\gamma_1 r_{1n}^{\;2}-1$, $c_{3n}=\dfrac{c_{2n}}{c_{1n}}$,

$c_{2n}=\left(\gamma_1 r_{1n}^{\;2}+M_0\right)a_1$, $c_{1n}=a_0+\gamma_1 r_{1n}^{\;2}+M_0$.

Correspondingly, simplifying $F_{1n}\left(q\right)$ by incorporating $\overline{\theta_H}\left(r_n,q\right)$, results

$$F_{1n}\left(q_1\right)=Gr\left(\left(\frac{J_1(r_{1n})}{r_{1n}q_1}-\frac{J_1(r_{1n})r_{1n}a_5}{r_{1n}^{\;2}\left(+a_4\right)}\right)\left(\frac{1}{c_{3n}}+\frac{c_{11n}}{q_1+c_{3n}}\right)\right), \tag{21}$$

where

$$c_{8n}=\frac{c_{7n}c_{6n}}{c_{3n}},\; c_{9n}=\frac{c_{7n}(c_{3n}-c_{6n})}{c_{3n}},\; c_{10n}=\frac{(a_1+a_3)a_3}{c_{3n}(a_3+c_{3n})},\; c_{11n}=c_{10n}-1,$$

$$F_{2n}(q_1)=\left(\frac{Q_{2n}}{q_1}-\frac{Q_{3n}}{q_1+c_{3n}}+Q_{4n}\frac{\omega}{q_1^2+\omega^2}+Q_{5n}\frac{q_1}{q_1^2+\omega^2}-\frac{Q_{6n}}{q_1+c_{3n}}\right)\frac{J_1(r_n)}{r_n}, \tag{22}$$

with

$$Q_{2n}=\frac{Q_{0n}c_{10n}}{\phi_1}, Q_{3n}=\frac{Q_{0n}(c_{10n}-1)}{\phi_1}, Q_{4n}=\frac{Q_{1n}c_{18n}}{\phi_1}, Q_{5n}=\frac{Q_{1n}c_{16n}}{\phi_1},$$

$$Q_{6n}=\frac{Q_{1n}c_{17n}}{\phi_1}, c_{12n}=a_1-c_{3n}, c_{13n}=\omega^2+a_1c_{3n},$$

$$c_{14n}=\omega^2+c_{3n}^{\;2}, c_{15n}=\frac{c_{12n}}{c_{14n}}, c_{16n}=\frac{c_{13n}}{c_{14n}}, c_{17n}=\frac{c_{12n}.c_{3n}}{c_{14n}}, c_{18n}=c_{15n}.\omega^2.$$

Incorporating Eqs. (20)-(22) into Eq. (19), we get:

$$\begin{aligned}\overline{e_{1H}}(r_{1n},q_1)&=\frac{J_1(r_{1n})}{r_{1n}q_1}+\frac{J_1(r_{1n})}{r_{1n}}\left(\frac{c_{8n}}{q_1}+\frac{c_{9n}}{q_1+c_{3n}}\right)\\&+Gr_1\frac{J_1(r_{1n})}{r_{1n}}\left(\left(\begin{array}{l}\frac{c_{23n}}{q_1}\\-\frac{c_{24n}}{q_1+c_{3n}}-\frac{c_{25n}}{q_1+a_{4n}}\end{array}\right)\right)+\left(\begin{array}{l}\frac{Q_{2n}}{q_1}-\frac{c_{26n}}{q_1+c_{3n}}\\+\frac{Q_{4n}\omega+Q_{5n}q}{q_1^2+\omega^2}\end{array}\right)\frac{J_1(r_{1n})}{r_{1n}}\end{aligned} \tag{23}$$

where

$$c_{19n}=\frac{c_{11n}}{c_{3n}}, c_{20n}=\frac{a_{5n}}{c_{3n}}, c_{21n}=\frac{1}{c_{3n}-a_{4n}}, c_{22n}=\frac{1}{c_{3n}+a_{4n}},$$

$$c_{23n}=\frac{1}{c_{3n}}+c_{19n}, c_{24n}=c_{19n}+c_{22n}, c_{25n}=c_{20n}+c_{21n}, c_{26n}=c_{3n}+c_{6n}$$

Laplace inverse of Eq. (23), gives

$$\begin{aligned}e_{1H}(r_{1n},\tau_1)&=\frac{J_1(r_{1n})}{r_{1n}}+\frac{J_1(r_{1n})}{r_{1n}}\left(c_{8n}+c_{7n}\,\mathrm{e}^{(-c_{3n}\tau_1)}\right)\\&+Gr_1\frac{J_1(r_{1n})}{r_{1n}}\left(\begin{array}{l}c_{23n}-c_{24n}\,\mathrm{e}^{(-c_{3n}\tau_1)}\\-c_{25n}\,\mathrm{e}^{(-a_{4n}\tau_1)}\end{array}\right)+\left(\begin{array}{l}Q_{2n}-c_{26n}\,\mathrm{e}^{(-c_{3n}\tau_1)}\\+Q_{4n}\sin(\omega\tau_1)\\+Q_{5n}\cos(\omega\tau_1)\end{array}\right)\frac{J_1(r_{1n})}{r_{1n}}.\end{aligned} \tag{24}$$

Now by taking Hankel inverse by

$$H_0^{-1}\left(u_H\left(r_{1n},\tau_1\right)\right)=w\left(r_1,\tau_1\right)=2\sum_{n=1}^{\infty}w_H\left(r_{1n},\tau_1\right)\frac{J_0\left(rr_{1n}\right)}{J_1\left(r_{1n}\right)},$$

Eq. (24) yields:

$$e_1\left(r_1,\tau_1\right)=1+2\sum_{n=1}^{\infty}\frac{J_0(rr_{1n})}{J_1(r_{1n})r_n}\left[Gr_1\begin{pmatrix}c_{23n}-c_{24n}e^{-c_{3n}\tau_1}\\-c_{25n}e^{-a_{4n}\tau_1}\end{pmatrix}+\begin{pmatrix}Q_{2n}-c_{26n}e^{-c_{3n}\tau_1}+Q_{4n}\sin\left(\omega\tau_1\right)\\+Q_{5n}\cos\left(\omega\tau_1\right)\end{pmatrix}\right]. \quad (25)$$

2.2 Atangana-baleanue fractional model

Now utilizing Atangana-Baleanue fractional derivative to Eqs. (7)-(8), yields:

$${}^{AB}\wp_t{}^{\alpha}e_1\left(r_1,\tau_1\right)=\frac{\left(\xi_0+\xi_1\cos\omega\tau_1\right)}{\phi_1}+\gamma_1\left(\frac{\partial^2 v\left(r_1,\tau_1\right)}{\partial r_1^2}+\frac{1}{r_1}\frac{\partial v\left(r_1,\tau_1\right)}{\partial r_1}\right)$$

$$-M_1 v\left(r_1,\tau_1\right)\pm Gr\theta\left(r_1,\tau_1\right), \quad (26)$$

$${}^{AB}\wp_t{}^{\alpha}\theta(r_1,\tau_1)=b_0\left(\frac{\partial^2\theta(r_1,\tau_1)}{\partial r_1^2}+\frac{1}{r_1}\frac{\partial\theta(r_1,\tau_1)}{\partial r_1}\right), \quad (27)$$

Eqs. (26) and (27) using conditions from Eq. (9) are solved by joint Laplace and Hankel transformations as follows:

2.2.1 Solution of the energy equation

Applying the joint Laplace and Hankel transforms using the transformed condition to Eq. (27), we get,

$$\overline{\theta_H}(r_{1n},q_1)=\frac{J_1(r_{1n})}{r_{1n}q_1}-\frac{a_{5n}\,r_{1n}\,J_1(r_{1n})}{r_{1n}^{\;2}\left(q_1^{\;\beta}+a_{4n}\right)}, \quad (28)$$

where $a_2=\dfrac{a_0}{b_0}, a_{3n}=a_2+r_{1n}^{\;2}, a_{4n}=\dfrac{a_1 r_{1n}^{\;2}}{a_{3n}}, \dfrac{a_1}{a_{3n}a_{4n}}=\dfrac{1}{r_{1n}^{\;2}}, a_{5n}=\dfrac{a_2}{a_2+r_{1n}^{\;2}}.$

Now applying inverse Laplace transformation to Eq. (28), and by using Lorenzo and Hartley's and Robotnov and Hartley's functions respectively [Ali, Imtiaz, Khan et al. (2018)]

$$L^{-1}\left(\frac{g^{-\upsilon}}{g^{\beta}+\chi}\right)=\Re_{\beta,\upsilon}\left(-\chi,\tau\right)=\sum_{n=0}^{\infty}\frac{\left(-\chi\right)^n\tau^{(n+1)\beta-1-\upsilon}}{\Gamma\{\left(n+1\right)\beta-\upsilon\}},$$

we get:

$$\overline{\theta_H}(r_{1n},\tau_1)=\frac{J_1(r_{1n})}{r_{1n}}-\frac{a_5\, r_{1n}\, J_1(r_{1n})}{{r_{1n}}^2}F_\beta\left(-a_4,\tau_1\right), \tag{29}$$

which upon inverse Hankel transform yields:

$$\theta(r_1,\tau_1)=1-2\sum_{n=1}^{\infty}\frac{J_0(rr_{1n})r_n a_5}{{r_n}^2\, J_1(r_{1n})}F_\beta\left(-a_4,\tau_1\right). \tag{30}$$

2.2.2 Solution of the velocity distribution

Applying the joint Hankel and Laplace transform to Eq. (26), we get:

$$\begin{aligned}\left(\frac{a_0{q_1}^\alpha}{{q_1}^\alpha+a_1}+M_1\right)\overline{e_{1H}}\left(r_{1n},q_1\right)&=\gamma_1\begin{pmatrix}-{r_{1n}}^2\overline{e_H}\left(r_{1n},q_1\right)\\+r_{1n}J_1(r_{1n})\overline{e}(1,q_1)\end{pmatrix}\\&+\frac{1}{\phi_1}\left(\frac{\xi_0}{q_1}+\frac{\xi_1}{{q_1}^2+\omega^2}\right)\frac{J_1\left(r_{1n}\right)}{r_{1n}}+Gr_1\,\overline{\theta}_H(r_{1n},q_1).\end{aligned} \tag{31}$$

Incorporating the transformed condition $\overline{e}(1,q_1)=\dfrac{1}{q_1}$, Eq. (31) becomes:

$$\overline{e_{1H}}\left(r_{1n},q_1\right)=\begin{pmatrix}\dfrac{\gamma_1 r_{1n}J_1(r_{1n})}{q_1}+Gr_1\,\overline{\theta}_H(r_{1n},q_1)\\+\dfrac{1}{\phi_1}\left(\dfrac{\xi_0}{q_1}+\dfrac{\xi_1}{{q_1}^2+\omega^2}\right)\dfrac{J_1\left(r_{1n}\right)}{r_{1n}}\end{pmatrix}\left(\frac{{q_1}^\alpha+a_1}{\begin{pmatrix}\left(a_0+\gamma_1{r_{1n}}^2+M_1\right){q_1}^\alpha\\+\left(\gamma_1{r_{1n}}^2+M_1\right)a_1\end{pmatrix}}\right). \tag{32}$$

Eq. (32) is simplified in the following form as:

$$\begin{aligned}\overline{e_{1H}}\left(r_{1n},q_1\right)&=\frac{J_1(r_{1n})}{r_{1n}q_1}+\frac{J_1(r_{1n})}{r_{1n}}\left(\frac{c_{8n}}{q_1}+\frac{c_{9n}}{{q_1}^\alpha+c_{3n}}\right)\\&+Gr_1\frac{J_1(r_{1n})}{r_{1n}}\left(\left(\frac{c_{23n}}{q_1}-\frac{c_{24n}}{{q_1}^\alpha+c_{3n}}-\frac{c_{25n}}{{q_1}^\alpha+a_{4n}}\right)\right)\\&+\left(\frac{Q_{2n}}{q_1}-\frac{c_{26n}}{{q_1}^\alpha+c_{3n}}+\frac{Q_{4n}\omega+Q_{5n}q}{{q_1}^2+\omega^2}\right)\frac{J_1\left(r_{1n}\right)}{r_{1n}}\end{aligned} \tag{33}$$

where

$$c_{7n}=\frac{c_{4n}}{c_{1n}},\ c_{6n}=\frac{c_{5n}}{c_{4n}}, c_{5n}=\gamma_1 r_{1n}{}^2 a_1-c_{3n},\ c_{4n}=\gamma_1 r_{1n}{}^2-1,\ c_{3n}=\frac{c_{2n}}{c_{1n}},$$

$$c_{2n}=\left(\gamma_1 r_{1n}{}^2+M_0\right)a_1,\ c_{1n}=a_0+\gamma_1 r_{1n}{}^2+M_0.$$

$$c_{8n}=\frac{c_{7n}c_{6n}}{c_{3n}},\ c_{9n}=\frac{c_{7n}(c_{3n}-c_{6n})}{c_{3n}},\ c_{10n}=\frac{\left(a_1+a_3\right)a_3}{c_{3n}\left(a_3+c_{3n}\right)},\ c_{11n}=c_{10n}-1,$$

$$\xi_{2n}=\frac{\xi_{0n}c_{10n}}{\phi_1}, \xi_{3n}=\frac{\xi_{0n}(c_{10n}-1)}{\phi_1}, \xi_{4n}=\frac{\xi_{1n}c_{18n}}{\phi_1}, \xi_{5n}=\frac{\xi_{1n}c_{16n}}{\phi_1},$$

$$\xi_{6n}=\frac{\xi_{1n}c_{17n}}{\phi_1}, c_{12n}=a_1-c_{3n}, c_{13n}=\omega^2+a_1c_{3n}, c_{14n}=\omega^2+c_{3n}{}^2,$$

$$c_{15n}=\frac{c_{12n}}{c_{14n}}, c_{16n}=\frac{c_{13n}}{c_{14n}}, c_{17n}=\frac{c_{12n}.c_{3n}}{c_{14n}}, c_{18n}=c_{15n}.\omega^2.$$

$$\begin{aligned}\overline{e_{1H}}\left(r_{1n},q_1\right)=&\frac{J_1(r_n)}{r_nq_1}+\frac{J_1(r_{1n})}{r_{1n}}\left(\frac{c_{8n}}{q_1}+\frac{c_{9n}}{q_1{}^{\beta}+c_{3n}}\right)\\&+Gr_1\frac{J_1(r_{1n})}{r_{1n}}\left(\left(\frac{c_{23n}}{q_1}-\frac{c_{24n}}{q_1{}^{\beta}+c_{3n}}-\frac{c_{25n}}{q_1{}^{\beta}+a_{4n}}\right)\right)\\&+\left(\frac{\xi_{2n}}{q_1}-\frac{c_{26n}}{q_1{}^{\beta}+c_{3n}}+\frac{\xi_{4n}\omega+\xi_{5n}q}{q_1{}^2+\omega^2}\right)\frac{J_1\left(r_{1n}\right)}{r_{1n}}\end{aligned}\tag{34}$$

where

$$c_{19n}=\frac{c_{11n}}{c_{3n}}, c_{20n}=\frac{a_{5n}}{c_{3n}}, c_{21n}=\frac{1}{c_{3n}-a_{4n}}, c_{22n}=\frac{1}{c_{3n}+a_{4n}},$$

$$c_{23n}=\frac{1}{c_{3n}}+c_{19n}, c_{24n}=c_{19n}+c_{22n},$$

$$c_{25n}=c_{20n}+c_{21n}, c_{26n}=c_{3n}+c_{6n}$$

Applying Laplace inverse to Eq. (34), we get:

$$e_{1H}\left(r_{1n},\tau_1\right)=\frac{J_1(r_{1n})}{r_{1n}}+\frac{J_1(r_{1n})}{r_{1n}}\left(c_{8n}+c_{7n}e^{-c_{3n}\tau_1}\right)$$
$$+Gr_1\frac{J_1(r_{1n})}{r_{1n}}\begin{pmatrix}c_{23n}-c_{24n}F_\beta\left(-c_{3n},\tau_1\right)\\-c_{25n}F_\beta\left(-a_{4n},\tau_1\right)\end{pmatrix} \tag{35}$$
$$+\begin{pmatrix}\xi_{2n}-c_{26n}F_\beta\left(-c_{3n},\tau_1\right)+\\\xi_{4n}\sin\left(\omega\tau_1\right)+\xi_{5n}\cos\left(\omega\tau_1\right)\end{pmatrix}\frac{J_1\left(r_{1n}\right)}{r_{1n}}$$

Now by taking Hankel inverse by the above-mentioned result, yields

$$e_1\left(r_1,\tau_1\right)=1+2\sum_{n=1}^{\infty}\frac{J_0(rr_{1n})}{J_1(r_{1n})r_{1n}}\left[\begin{array}{l}Gr_1\begin{pmatrix}c_{23n}-c_{24n}F_\beta\left(-c_{3n},\tau_1\right)\\-c_{25n}F_\beta\left(-a_{4n},\tau_1\right)\end{pmatrix}\\+\begin{pmatrix}\xi_{2n}-c_{26n}F_\beta\left(-c_{3n},\tau_1\right)\\+\xi_{4n}\sin\left(\omega\tau_1\right)+\xi_{5n}\cos\left(\omega\tau_1\right)\end{pmatrix}\end{array}\right]. \tag{36}$$

3 Heat transfer rate

The dimensional expression of the rate of heat transfer in $\left(r_1,\theta_1,z\right)$ is given by

$$\text{Nu}=-\frac{R_0k_{nf}}{\left(T_w-T_\infty\right)k_f}\left(\frac{\partial\theta\left(r_1,t_1\right)}{\partial r_1}\right)_{r_1=1}. \tag{37}$$

Using the dimensionless variables from Eq. (6), the non-dimensional form of heat transfer rate by ignoring the * notation is given as

$$\text{Nu}=-\frac{k_{nf}}{k_f}\left(\frac{\partial\theta\left(r_1,\tau_1\right)}{\partial r_1}\right)_{r_1=1} \tag{38}$$

4 Graphical interpretation and discussion

The Casson blood flow is assumed with the gold nanoparticles in cylindrical coordinates. The classical model is transformed into fractional models by Caputo-Fabrizio and Atangana-Balenu time-fractional operators and by joint Laplace and Hankel transforms the exact solutions have been found. Various physical parameters effect on temperature $\theta\left(r_1,\tau_1\right)$ and velocity $e_1\left(r_1,\tau_1\right)$ profiles have been deliberated physically. Fig. 1 shows the physical model of the problem. Fig. 2 has been plotted for the involvement of α on temperature profile. It is worthwhile that at the centre of the cylinder when α increases the fractional fluid temperature is observed higher while to the cylinder walls the reverse effect has been perceived.

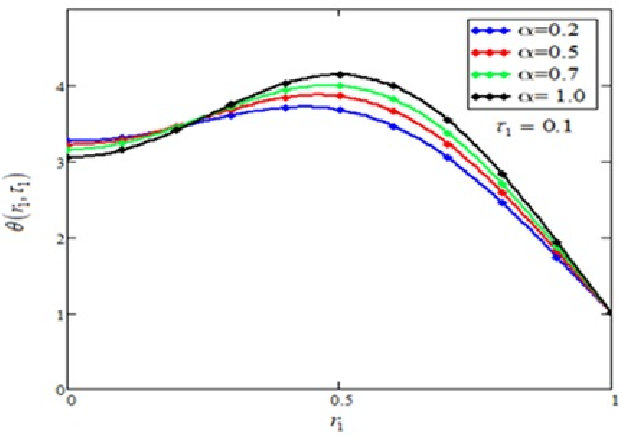

Figure 2: Temperature profile for different values of α, when $\omega = 0.1$, $Gr = 0.5$, $\gamma = 1$, $M = 1$ & $\Pr = 22.64$

Fig. 3 is plotted to show the effect of the volume fraction ϕ on the temperature profile. It can be seen from the figure that fluid temperature increases by taking higher values ϕ. This enhancement of the fluid temperature b the shear-thinning behaviour of the nanoparticles.

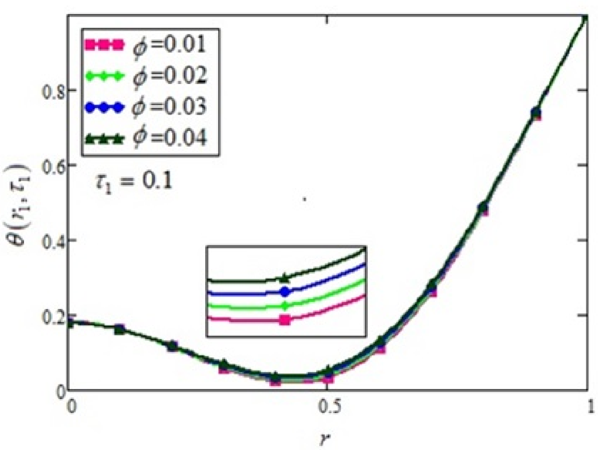

Figure 3: Temperature profile for different values of ϕ, when $\omega = 0.1$, $Gr = 0.5$, $\gamma = 1$, $M = 1$ $\Pr = 22.64$

Fig. 4 illustrates the behaviour of the Nusselt number. By increasing ϕ the Nusselt number is increased which indicates a rise in heat transfer rate.

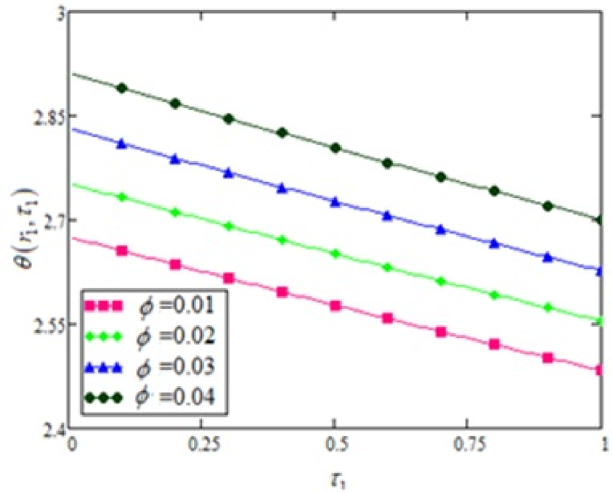

Figure 4: Variation in Nusselt number for different values of ϕ, when $\omega = 0.1$ $Gr = 0.5, \gamma = 1,\ M = 1\ \&\ \Pr = 22.64$

The effect of nanoparticle volume fraction ϕ and time t on Nusselt number has been noticed in Tab. 2. It is observed that an increase in the values of ϕ and τ_1 enhancement in Nusselt number occurs.

Table 2: Effect of various parameters on Nusselt number (Nu)

ϕ	τ_1	Nu
0.01	1	0.176
0.04	1	0.182
0.01	**1.5**	0.18

From Tab. 3 it is found that the heat transfer rate of Blood-based nanofluid with gold nanoparticles is 4% greater than fluid without nanoparticles.

Table 3: Impact of volume fraction on nusselt number and percent enhancement

ϕ	τ_1	**Nu**	**%**
0	1	0.175	-
0.01	1	0.176	0.571
0.02	1	0.177	1.142
0.03	1	0.179	2.28
0.04	1	0.182	4

Figs. 5-8, show the effect of the fractional parameter α on velocity profiles. It has been observed from these figures that for higher values of α, fluid velocity decreases. The corresponding results for regular blood flow with gold nanoparticles ($\alpha = 1$) are compared and found that regular blood is more viscous than the fractional blood velocity.

Fig. 5 shows the effect of the Casson fluid parameter γ on fractionalized fluid velocity. In Fig. 5(a), Casson fluid parameter $\gamma = 0.5$ whereas in Fig. 5(b), $\gamma = 1$. From this figure, it is depicted that by increasing γ from 0.5 to 1, the fluid velocity increases. Substantially it is true because increasing γ the yield stress falls through which boundary layer thickness decreases.

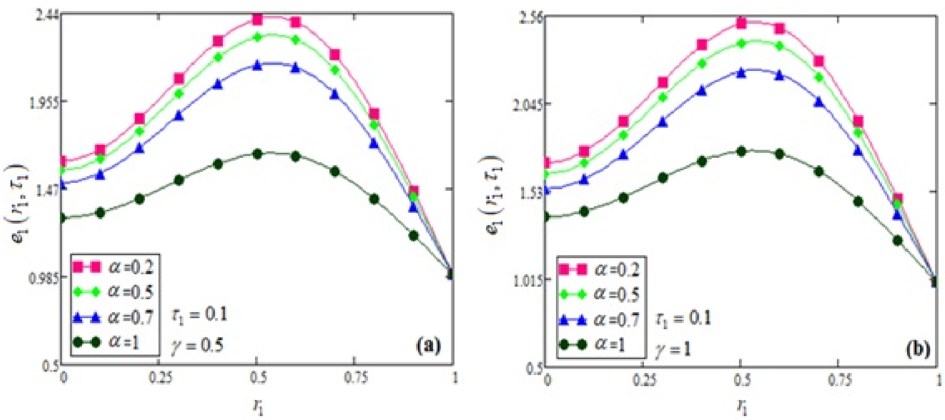

Figure 5: Velocity profile for different values of γ, when $\omega = 0.1$, $M = 1,\ \phi = 0.01,\ Gr = 0.5\ \&\ \Pr = 22.64$

The influence of Gr fluid velocity has been discussed in Fig. 6. In Fig. 6(a) Grashoff number is Gr=0.5 whereas in Fig. 6(b) Gr=1, it is seen that the velocity increases with an increase in Gr due to enhancement of buoyancy forces. From Gr and γ, it can be concluded that by enhancing both parameters the blood velocity increases and through this the cancer tumour can be targeted through gold Nanoparticles and easily destroyed without harming other healthy tissues.

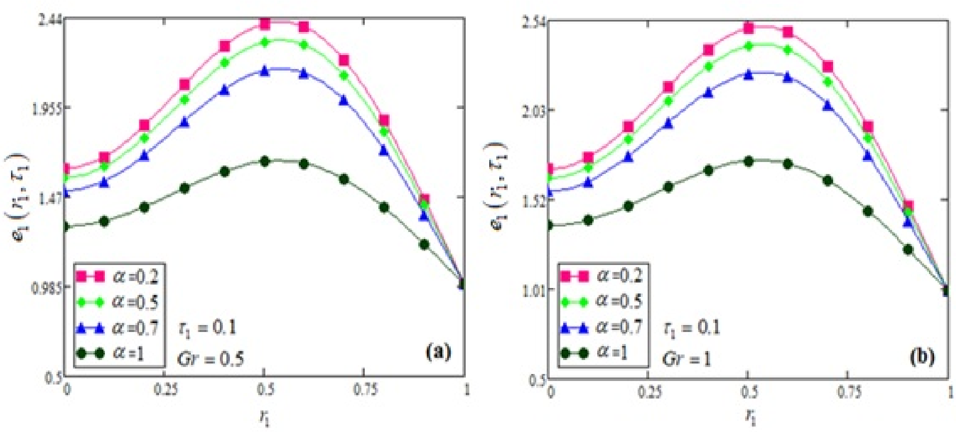

Figure 6: Velocity profile for different values of Gr, when $\omega = 0.1$, $M = 1,\ \gamma = 1,\ \phi = 0.01\ \&\ \Pr = 22.64$

Fig. 7 depicts the effect of nanoparticle volume fraction ϕ. In Fig. 7(a) volume fractions are $\phi = 0.01$ whereas in Fig. 7(b) $\phi = 0.04$. From this figure, it is determined that by enhancing ϕ from 0.01 to 0.04, the fluid becomes more viscous which leads to decrease velocity.

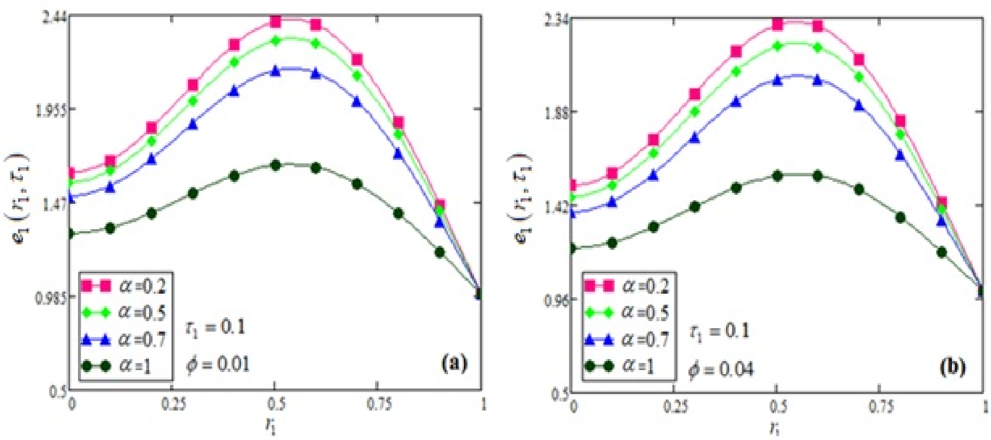

Figure 7: Velocity profile for different values of ϕ, when $\omega = 0.1$, $M = 1$, $\gamma = 1$, $Gr = 0.5$ & $\Pr = 22.64$

In Fig. 8 the effect of magnetic field parameter M has been shown. In Fig. 8(a) magnetic field parameter is M=1 whereas in Fig. 8(b) M=2 It is found from the figure that by increasing M the velocity profile decreases. Physically, when a magnetic field is applied the Lorentz forces produce as an external force, which retards blood flow. A decreased in fluid velocity means the viscosity of the fluid (blood) is increased which consequently maintains the laminarity of the flow.

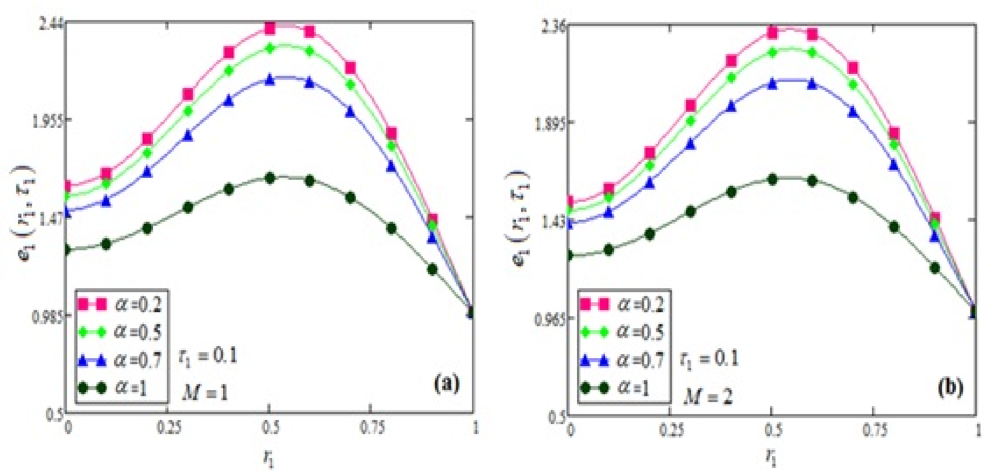

Figure 8: Velocity profile for different values of M, when $\omega = 0.1$, $Gr = 0.5$, $\gamma = 1$, $\phi = 0.01$ & $\Pr = 22.64$

Fig. 9 shows the comparison of two well-known fractional derivatives It has been observed from the figure that the velocity by AB derivative higher than the CF derivative velocity.

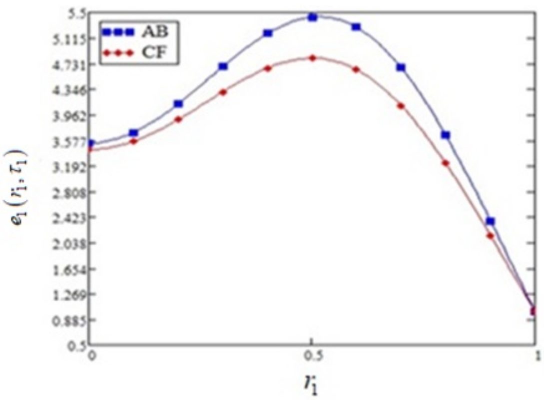

Figure 9: Comparison of AB and CF derivatives

Fig. 10 shows the velocities of two different fractional derivatives (AB and CF) which are compared for different values of *t*. It has been observed that for initial values of time velocity of AB is greater than CF and by increasing *t* an invert behaviour has been seen. While for the unit time both velocities become indistinguishable.

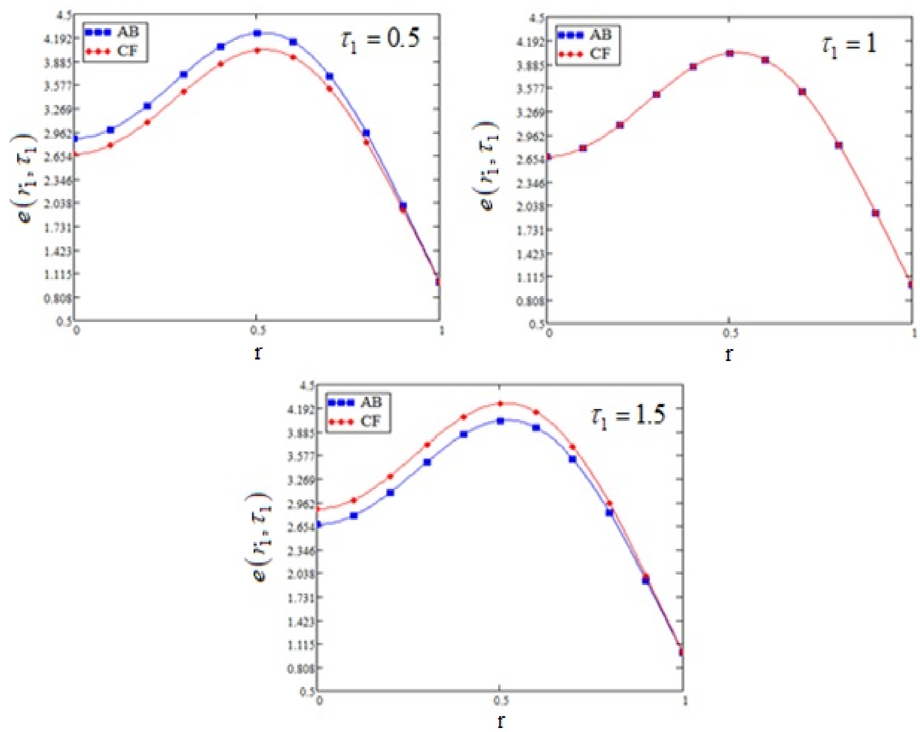

Figure 10: Comparison of AB and CF velocities for different times

5 Conclusions

A comparative study for unsteady Nanofluid blood flow is carried out in cylindrical coordinates. The influence of various physical parameters on fluid velocity in the cylindrical field has been shown. Closed-form solutions have been obtained by utilizing the Joint Laplace and Hankel transforms. On the basis of the obtained results, it has been concluded that for different times the velocities of both fractional operators show opposite behavior and for a unit time, both velocities become indistinguishable. The AB fractional operator is more dominant in blood velocity as compared to the CF fractional operator and an accelerating behavior has been noticed for the fluid flow by AB fractional operator as compared to the CF operator which is a key thing for the consideration. The blood velocity increases with an increase in the Grashoff number Gr and Casson fluid parameter γ, the blood velocity increases due to the shear-thinning behavior of the blood and rapidly carries the gold nanoparticles to the cancerous tumor. Correspondingly, an external applied magnetic field M retards the velocity of the fluid and controls the turbulency produced in the blood flow.

Acknowledgement: The research is supported by Universiti Teknologi PETRONAS YUTP Grant (Cost Center 015LC0-173). Special thanks to staffs who have contributed either directly or indirectly to the research.

Funding Statement: The funding is sponsored by Universiti Teknologi PETRONAS YUTP Grant (Cost Center 015LC0-173).

Conflicts of Interest: The authors declare that they have no conflicts of interest to report regarding the present study.

References

Abdelhalim, M. A. K.; Jarrar, B. M. (2011): The appearance of renal cells cytoplasmic degeneration and nuclear destruction might be an indication of GNPs toxicity. *Lipids in Health and Disease*, vol.10, no. 1, pp. 147.

Agostinelli, E.; Vianello, F.; Magliulo, G.; Thomas, T.; Thomas, T. J. et al. (2015): Nanoparticle strategies for cancer therapeutics: nucleic acids, polyamines, bovine serum amine oxidase and iron oxide nanoparticles. *International Journal of Oncology*, vol. 46, no. 1, pp. 5-16.

Ali, F.; Imtiaz, A.; Khan, I.; Sheikh, N. A. (2018): The flow of magnetic particles in blood with isothermal heating: a fractional model for two-phase flow. *Journal of Magnetism and Magnetic Materials*, vol. 456, pp. 413-422.

Ali, F.; Yousaf, S.; Khan, I.; Sheikh, N. A. (2019): A new idea of Atangana-Baleanu time-fractional derivatives to blood flow with magnetic particles in a circular cylinder: two-phase flow model. *Journal of Magnetism and Magnetic Materials*, vol. 486, no. 165282, pp. 1-10.

Aman, S.; Khan, I.; Ismail, Z.; Salleh, M. Z. (2018): Impacts of gold nanoparticles on MHD mixed convection poiseuille flow of nanofluid passing through a porous medium in the presence of thermal radiation, thermal diffusion and chemical reaction. *Neural Computing and Applications*, vol. 30, no. 3, pp. 789-797.

Ashizawa, A. T.; Cortes, J. (2015). Liposomal delivery of nucleic acid-based anticancer therapeutics: BP-100-1.01. *Expert Opinion on Drug Delivery*, vol. 12, no. 7, pp. 1107-1120.

Atangana, A. (2016): Derivative with two fractional orders: a new avenue of investigation toward revolution in fractional calculus. *The European Physical Journal Plus*, vol. 131, no. 10, pp. 373.

Atangana, A. (2017a): Fractal-fractional differentiation and integration: connecting fractal calculus and fractional calculus to predict complex system. *Chaos, Solitons & Fractals*, vol. 102, pp. 396-406.

Atangana, A. (2017b): *Fractional Operators with Constant and Variable Order with Application to Geo-Hydrology*. Academic Press, USA.

Atangana, A.; Baleanu, D. (2016): New fractional derivatives with the nonlocal and non-singular kernel: theory and application to heat transfer model. *arXiv preprint arXiv:*1602.03408.

Daniel, M. C.; Astruc, D. (2004): Gold nanoparticles: assembly, supramolecular chemistry, quantum-size-related properties, and applications toward biology, catalysis, and nanotechnology. *Chemical Reviews*, vol. 104, pp. 293-346.

Ghosh, P.; Han, G.; De, M.; Kim, C. K.; Rotello, V. M. et al. (2008): Gold nanoparticles in delivery applications. *Advanced Drug Delivery Reviews*, vol. 60, no. 11, pp. 1307-1315.

Hatami, M.; Hatami, J.; Ganji, D. D. (2014): Computer simulation of MHD blood conveying gold nanoparticles as a third grade non-Newtonian nanofluid in a hollow porous vessel. *Computer Methods and Programs in Biomedicine*, vol. 113, no. 2, pp. 632-641.

Herzog, H. (1998): History of tuberculosis. *Respiration*, vol. 65, no. 1, pp. 5.

Ho, B. N.; Pfeffer, C. M.; Singh, A. T. (2017): Update on nanotechnology-based drug delivery systems in cancer treatment. *Anticancer Research*, vol. 37, no. 11, pp. 5975-5981.

Hussein, S. I.; Sultan, A. S.; Yaseen, N. Y. (2016): Gold nanoparticles for photothermal therapy of cancerous cells *in vitro*. *International Journal of Current Microbiology and Applied Sciences*, vol. 5, no. 10, pp. 261-266.

Iancu, C. (2013): Photothermal therapy of human cancers (PTT) using gold nanoparticles. *Biotechnology*, *Molecular Biology and Nanomedicine*, vol. 1, pp. 53-60.

Ikram, A.; Jamil, Y.; Ahmad, T.; Ikram, H.; Ameen, A. et al. (2019): Controllable fabrication and characterization of gold nanoparticles: enhanced therapeutic approaches in cancer. *Open Journal of Science and Technology*, vol. 2, no. 1, pp. 26-28.

Kong, F. Y.; Zhang, J. W.; Li, R. F.; Wang, Z. X.; Wang, W. J. et al. (2017): Unique roles of gold nanoparticles in drug delivery, targeting and imaging applications. *Molecules*, vol. 22, no. 9, pp. 1445.

Leech, D. P.; Scott, J. T. (2017): Nanotechnology documentary standards. *The Journal of Technology Transfer*, vol. 42, no. 1, pp. 78-97.

Mandal, P. K. (2005): An unsteady analysis of non-Newtonian blood flow through tapered arteries with stenosis. *International Journal of Non-Linear Mechanics*, vol. 40, no. 1, pp. 151-164.

Owolabi, K. M.; Atangana, A. (2018): Chaotic behavior in a system of noninteger-order ordinary differential equations. *Chaos, Solitons & Fractals*, vol. 115, pp. 362-370.

Owolabi, K. M.; Atangana, A. (2019): On the formulation of Adams-Bashforth scheme with Atangana-Baleanu-Caputo fractional derivative to model chaotic problems. *Chaos: An Interdisciplinary Journal of Nonlinear Science*, vol. 29, no. 2, pp.1-12.

Oztop, H. F.; Abu-Nada, E. (2008): Numerical study of natural convection in partially heated rectangular enclosures filled with nanofluids, *International Journal Heat Fluid Flow*, vol. 29, no. 5, pp. 1326-1336.

Pavlova, N. N.; Thompson, C. B. (2016): The emerging hallmarks of cancer metabolism. *Cell Metabolism*, vol. 23, no. 1, pp. 27-47.

Rudramurthy, G. R.; Swamy, M. K. (2018): Potential applications of engineered nanoparticles in medicine and biology: an update. *Journal of Biological Inorganic Chemistry*, vol. 23, no. 8, pp. 1185-1204.

Saallah, S.; Lenggoro, I. W. (2018): Nanoparticles carrying biological molecules: recent advances and applications. *KONA Powder and Particle Journal*, vol. 35, pp. 89-111.

Shilo, M.; Berenstein, P.; Dreifuss, T.; Nash, Y.; Goldsmith, G. et al. (2015): Insulin-coated gold nanoparticles as a new concept for personalized and adjustable glucose regulation. *Nanoscale*, vol. 7, no. 48, pp. 20489-20496.

Srinivas, S.; Kothandapani, M. (2009): The influence of heat and mass transfer on MHD peristaltic flow through a porous space with compliant walls. *Applied Mathematics and Computation*, vol. 213, no. 1, pp. 197-208.

Tomar, A.; Garg, G. (2013): A short review on the application of gold nanoparticles. *Global Journal of Pharmacology*, vol. 7, no. 1, pp. 34-38.

Wang, J. (2003): Nanoparticle-based electrochemical DNA detection. *Analytica Chimica Acta*, vol. 500, no. 1-2, pp. 247-257.

Yao, C.; Zhang, L.; Wang, J.; He, Y.; Xin, J. et al. (2016): Gold nanoparticle-mediated phototherapy for cancer. *Journal of Nanomaterials*, vol. 2016, no. 5497136, pp. 1-29.

Nomenclature

p	oscillating pressure gradient	ϕ	solid volume fraction of nanoparticle;
P_0	amplitude of the systolic pressure gradient	ρ_f	density of base fluid (kg m^{-3});
P_1	amplitude of the diastolic pressure gradient	ρ_{nf}	density of Nanofluid (kg m^{-3});
e_1	dimensionless fluid velocity in z'-direction (m/s);	$(\rho c_p)_f$	heat capacitance of base fluid;
r_1	radial axis	$(\rho c_p)_{nf}$	heat capacitance of Nanofluid;
v_f	dynamic viscosity coefficient of base fluid;	$(\rho c_p)_s$	heat capacitance of nanoparticle;
Gr	Grashoff number	μ_f	viscosity of base fluid (kg m^{-1} s^{-1});
k_f	thermal conductivity of base fluid ($Wm^{-1}K^{-1}$);	σ_f	electrical conductivity of base fluid (=s^3 A^2 $m^{-3}kg^{-1}$);
k_{nf}	thermal conductivity of Nanofluid ($Wm^{-1}K^{-1}$);	σ_{nf}	electrical conductivity of Nanofluid (=s^3 A^2 $m^{-3}kg^{-1}$);
k_s	thermal conductivity of nanoparticles ($Wm^{-1}K^{-1}$);	σ_s	electrical conductivity of nanoparticle (=s^3 A^2 $m^{-3}kg^{-1}$).
μ_{nf}	dynamic viscosity of Nanofluid (kg m^{-1} s^{-1});	γ	Casson fluid parameter;
τ_1	dimensionless time	ρ_s	density of the solid particles
T	fluid temperature (K);	M	Magnetic parameter;
β_f	thermal expansion coefficient of base fluid (K^{-1});	ω	angular frequency
β_{nf}	thermal expansion coefficient of Nanofluid (K^{-1});	Pr	Prandtl number;
β_s	thermal expansion coefficient of nanoparticle (K^{-1});	B_0	induced magnetic field;
R_0	radius of the cylinder	g	acceleration due to gravity (m s^{-2});
u_0	characteristic velocity	t_1	dimensional time
v_{nf}	kinematic viscosity of the nanofluid	T_∞	ambient temperature
α	fractional parameter	T_w	wall temperature